

## Evaluation of Kubo's Formula for the Impurity Resistance of an Interacting Electron Gas\*

J. S. LANGER†

*University of California, San Diego, La Jolla, California*

(Received January 25, 1962)

The impurity resistance of an interacting electron gas is evaluated at low but finite temperatures. Analytic techniques similar to those developed by the author for use in the zero-temperature problem are applied to the complete Kubo formula. The calculations are exact to all orders in the electron-electron interactions and to lowest order in the concentration of impurities. To lowest order in the temperature the conductivity is given correctly by the independent quasi-particle model. Corrections of order  $T^2$  are discussed in detail. It is shown that the only nonvanishing term of this order which explicitly contains the correlation between two quasi-particles is independent of the impurity concentration, and thus may almost always be neglected.

### I. INTRODUCTION

THIS paper is the third in a series devoted to an investigation of the transport properties of a normal, interacting electron gas. In the previous papers<sup>1,2</sup> the impurity resistance of this gas was computed at absolute zero temperature. The result was exact to all orders in the electron-electron and electron-impurity interactions and to lowest order in the concentration of impurities. The main purpose of the present paper is the formulation of this theory at finite temperatures. In particular, we shall apply techniques similar to those developed in I, II, and A to the evaluation of Kubo's formal expression for the transport coefficient,<sup>3</sup> and shall show that the zero-temperature limit of this calculation yields the previous result. In addition, we shall examine in detail some of the finite temperature corrections. The thermal conductivity of this system also has been investigated; and a proof of the Weidemann-Franz law will appear in a subsequent publication.

The Kubo formula probably provides the most rigorous possible point of departure for transport theory. Despite its extremely formal appearance, it has in fact proved amenable to direct evaluation for some simple models. Edwards,<sup>4</sup> and Chester and Thellung<sup>5</sup> have used the Kubo formula (or its equivalent) to calculate the impurity resistance of a system of independent electrons, and have recovered the usual solution of the linearized Boltzmann equation. Verboven<sup>6</sup> has extended this work to higher orders in the concentration of impurities and has found corrections to the conductivity not ordinarily derived via Boltzmann techniques. It would seem, however, that the Kubo formula might be most fruitfully applied in the full many-body

problem where it is not clear that any Boltzmann formulation is valid. Detailed prescriptions for perturbation expansions in quantum statistics have been developed within the last few years in papers by Montroll and Ward,<sup>7</sup> Bloch and De Dominicis,<sup>8</sup> and Luttinger and Ward.<sup>9</sup> Although transport coefficients are somewhat more complicated than the partition function, many-body techniques of the above kind must be applicable to nonequilibrium problems. Attempts in this direction have been made by Montroll and Ward,<sup>10</sup> and more recently by Konstantinov and Perel,<sup>11</sup> and Izuyama.<sup>12</sup> A somewhat different approach to the problem has been presented by Martin and Schwinger.<sup>13</sup>

Before going on to the detailed formalism to be presented here, let us review briefly some of the more important physical features of the previous work. The most striking result, as stated at the end of paper II, is that the zero-temperature, zero-frequency conductivity is given *exactly* by Landau's quasi-particle description of the Fermi fluid.<sup>14</sup> In other words, the single-particle picture of the low-lying excitations of a many-Fermion system turns out to be a direct consequence of the general structure of many-body perturbation theory. This is not really very surprising, especially in view of recent work by Luttinger<sup>15</sup> and Klein<sup>16</sup> on various equilibrium properties of the Fermi fluid. It is not immediately obvious, however, that the simple picture applies equally well to nonequilibrium properties.

The dynamical properties of a quasi-particle are determined by the behavior of the single-particle

\* Supported in part by the Office of Naval Research.

† Permanent address: Carnegie Institute of Technology, Pittsburgh 13, Pennsylvania.

<sup>1</sup> J. S. Langer, Phys. Rev. **120**, 714 (1960); **124**, 1003 (1961). These papers are hereafter referred to as I and II, respectively.

<sup>2</sup> Some mathematical techniques used in II are developed by the author in Phys. Rev. **124**, 997 (1961), hereafter referred to as A.

<sup>3</sup> R. Kubo, J. Phys. Soc. Japan **12**, 570 (1957).

<sup>4</sup> S. F. Edwards, Phil. Mag. **3**, 33, 1020 (1958).

<sup>5</sup> G. V. Chester and A. Thellung, Proc. Phys. Soc. (London) **73**, 745 (1959).

<sup>6</sup> E. Verboven, Physica **26**, 1091 (1960).

<sup>7</sup> E. Montroll and J. C. Ward Phys. Fluids **1**, 55 (1958).

<sup>8</sup> C. Bloch and C. De Dominicis, Nuclear Phys. **7**, 459 (1958); **10**, 181 (1959).

<sup>9</sup> J. M. Luttinger and J. C. Ward, Phys. Rev. **118**, 1417 (1960).

<sup>10</sup> E. Montroll and J. C. Ward, Physica **25**, 423 (1959).

<sup>11</sup> O. V. Konstantinov and V. I. Perel, Sov. Phys.—JETP **12**, 142 (1961).

<sup>12</sup> T. Izuyama, Progr. Theoret. Phys. (Kyoto) **25**, 964 (1961).

<sup>13</sup> P. C. Martin and J. Schwinger, Phys. Rev. **115**, 1342 (1959).

<sup>14</sup> L. D. Landau, Sov. Phys.—JETP **3**, 920 (1956); **5**, 101 (1957). See also A. A. Abrikosov and I. M. Khalatnikov, Sov. Phys. Uspekhi **66** (1), 68 (1958).

<sup>15</sup> J. M. Luttinger, Phys. Rev. **119**, 1153 (1960); **121**, 1251 (1961).

<sup>16</sup> A. Klein, Phys. Rev. **121**, 950 (1960); **121**, 957 (1960).

propagator in the neighborhood of its pole on the unphysical sheet of the complex energy plane. This pole occurs at the point  $\omega_{\mathbf{k}}$  which satisfies the equation

$$\epsilon_{\mathbf{k}} - \omega_{\mathbf{k}} - \Sigma'(\mathbf{k}, \omega_{\mathbf{k}}) = 0, \quad (1.1)$$

$\Sigma'$  being the proper self-energy function. We identify the real part of  $\omega_{\mathbf{k}}$  with the energy of the quasi-particle and the imaginary part with its rate of decay. A quasi-particle always carries a charge  $e$  equal to the charge of a single electron. When there is a finite concentration of impurities in the system, a quasi-particle must take the form of a wave packet localized within the mean free path. Because the background medium is fixed by the impurities, the current associated with a quasi-particle is given by the group velocity, i.e.,

$$\mathbf{J}_{\mathbf{k}} = e d\omega_{\mathbf{k}}/d\mathbf{k} = e\mathbf{u}_{\mathbf{k}}. \quad (1.2)$$

It may then be shown that the conductivity is

$$\sigma = n_e e^2 \tau / m^*, \quad (1.3)$$

where  $n_e$  is the number of electrons per unit volume, and  $m^*$  is the effective mass at the Fermi surface defined by

$$m^* \left. \frac{d\omega_{\mathbf{k}}}{d\mathbf{k}} \right|_{\mathbf{k}=\mathbf{k}_F} = \mathbf{k}_F. \quad (1.4)$$

The relaxation time  $\tau$  may be written in the form

$$\tau^{-1} = n_i u(k_F) \int_0^\pi \sigma(\theta) (1 - \cos\theta) 2\pi \sin\theta d\theta, \quad (1.5)$$

where  $n_i$  is the concentration of impurities and  $\sigma(\theta)$  is the differential cross section for scattering of a single quasi-particle by a single impurity. [Equation (1.5) is equivalent to Eq. (3.31) in II if we understand that the correct scattering amplitude is  $N(k_F)t^+$ .]

The scheme of the present paper is as follows. In Sec. II we start with Kubo's formula and derive a prescription for the evaluation of the conductivity via perturbation theory. This prescription is simpler than

those developed by the authors mentioned above,<sup>10-12</sup> and lends itself to an analysis in terms of reduced graphs of the sort discussed in A. The extension of these analytic techniques to the finite-temperature problem is presented in Sec. III. In Sec. IV we apply these techniques to the evaluation of the conductivity and show that Eq. (1.3) is the zero temperature limit of this theory. Finally, in Sec. V we examine corrections to the conductivity to order  $T^2$ .

## II. KUBO FORMULA

We start with Kubo's exact formula for the conductivity tensor<sup>3</sup>

$$\sigma_{ij}(\omega) = \frac{1}{\Omega} \int_0^\infty dt \int_0^\beta d\lambda \text{Tr}\{\rho_0 J_j(0) J_i(t+i\lambda)\} e^{-i\omega t}, \quad (2.1)$$

where  $J_i$  is the current operator,

$$J_i = (e/m) \sum_{\mathbf{k}} k_i a_{\mathbf{k}}^\dagger a_{\mathbf{k}}; \quad (2.2)$$

and

$$J_i(t) = e^{iHt} J_i e^{-iHt}. \quad (2.3)$$

$\rho_0$  is the equilibrium density matrix,

$$\rho_0 = (1/Z) e^{-\beta(H-\mu N)}; \quad Z = \text{Tr} e^{-\beta(H-\mu N)}, \quad (2.4)$$

$H$  being the Hamiltonian for the system of electrons and impurities, but excluding the external electric field.  $a_{\mathbf{k}}^\dagger$  and  $a_{\mathbf{k}}$  are the creation and annihilation operators for an electron of momentum  $\mathbf{k}$ .  $\mu$  is the chemical potential;  $\beta = 1/k_B T$  where  $k_B$  is Boltzmann's constant; and  $\Omega$  is the volume of the system. We use units in which  $\hbar = 1$ .

The integrand in Eq. (2.1) is essentially an auto-correlation coefficient which must vanish for sufficiently large values of the time  $t$  if the system is to have a finite conductivity. In other words, because of the presence of the impurities, any current fluctuation which occurs in the system will decay. With this assumption we may immediately perform the  $\lambda$  integration in Eq. (2.1). We integrate over  $t$  by parts and note that the quantity in brackets is a function only of  $t+i\lambda$ :

$$\begin{aligned} \sigma_{ij}(\omega) &= \frac{1}{\Omega} \int_0^\infty dt \left( \frac{e^{-i\omega t} - 1}{i\omega} \right) \int_0^\beta d\lambda \frac{\partial}{\partial t} \text{Tr}\{\rho_0 J_j(0) J_i(t+i\lambda)\} \\ &= -\frac{1}{\Omega} \int_0^\infty dt \left( \frac{e^{-i\omega t} - 1}{\omega} \right) \int_0^\beta d\lambda \frac{\partial}{\partial \lambda} \text{Tr}\{\rho_0 J_j(0) J_i(t+i\lambda)\} \\ &= -\frac{1}{\Omega} \int_0^\infty dt \left( \frac{e^{-i\omega t} - 1}{\omega} \right) \text{Tr}\{\rho_0 J_j(0) [J_i(t) - J_i(t+i\beta)]\}. \end{aligned} \quad (2.5)$$

From (2.3) and (2.4) we know that

$$\text{Tr}\{\rho_0 J_j(0) J_i(t+i\beta)\} = \text{Tr}\{\rho_0 J_i(t) J_j(0)\}; \quad (2.6)$$

thus

$$\sigma_{ij}(\omega) = -\frac{1}{\Omega} \int_0^\infty dt \left( \frac{e^{-i\omega t} - 1}{\omega} \right) \text{Tr}\{\rho_0 [J_i(t), J_j(0)]\}. \quad (2.7)$$

This form for  $\sigma$  was first derived by Verboven.<sup>6,17</sup> In

<sup>17</sup> This simple derivation of Verboven's result is due to J. M. Radcliffe.

all of the following work we shall consider only the dc conductivity of an isotropic system. In this case we define

$$\sigma = \sum_{i=1}^3 \sigma_{ii}(0) = -(2/3\Omega) \text{Im} \int_0^\infty dt \text{Tr}\{\rho_0 \mathbf{J}(t) \cdot \mathbf{J}(0)\}. \quad (2.8)$$

From this point on, our formal development proceeds in close analogy with that of II, Sec. II. We define the

function

$$\mathfrak{F}(t) \equiv \text{Tr}\{\rho_0 T[\mathbf{J}(t) \cdot \mathbf{J}(0)]\}, \quad (2.9)$$

where  $T$  is the usual time-ordering operator. Because only positive values of  $t$  occur in (2.8),  $\mathfrak{F}$  is the same as the integrand in the conductivity formula. It is  $\mathfrak{F}$ , however, which is most conveniently evaluated in terms of Feynman diagrams.

Let  $F(\nu)$  be the Fourier transform of  $\mathfrak{F}$

$$F(\nu) = \frac{1}{2\pi} \lim_{\eta \rightarrow 0} \int_{-\infty}^{\infty} \mathfrak{F}(t) e^{i\nu t - \eta |t|} dt. \quad (2.10)$$

$F(\nu)$  has the spectral representation:

$$F(\nu) = \frac{1}{2\pi i} \int_{-\infty}^{\infty} \rho(\nu') \left\{ \frac{1}{\nu' - \nu - i\eta} + \frac{1}{\nu' + \nu - i\eta} \right\} d\nu'; \quad (2.11)$$

where

$$\rho(\nu) = \frac{1}{Z} \sum_{n,m} e^{-\beta(E_n - \mu N_n)} \times |\langle n | \mathbf{J} | m \rangle|^2 \delta(E_m - E_n - \nu), \quad (2.12)$$

$|n\rangle$  and  $|m\rangle$  being eigenstates of  $H$  with eigenenergies  $E_n$  and  $E_m$ , respectively. Equations (2.11) and (2.12) are easily derived by inserting the complete set of states  $|n\rangle$ ,  $|m\rangle$ , etc., into (2.9) and evaluating the Fourier transform (2.10) explicitly. Notice that, unlike the analogous function defined in II,  $\rho$  is continuous from  $\nu = -\infty$  to  $+\infty$ . We may expect the value of  $\rho$  to be considerable for values of  $\nu$  greater than  $-k_B T$ , the negative values corresponding to the fact that a system at a finite temperature can emit energy. In the limit  $T \rightarrow 0$ ,  $\rho$  vanishes for  $\nu < 0$  and has a discontinuous derivative at  $\nu = 0$ .

Inversion of the Fourier transform for  $t > 0$  yields

$$\mathfrak{F}(t) = \int_{-\infty}^{\infty} F(\nu) e^{-i\nu t} d\nu = \int_{-\infty}^{\infty} \rho(\nu) e^{-i\nu t} d\nu, \quad t > 0. \quad (2.13)$$

The conductivity  $\sigma$  now may be expressed very simply in terms of  $\rho$ .

$$\begin{aligned} \sigma &= -\frac{2}{3\Omega} \text{Im} \int_0^{\infty} t dt \mathfrak{F}(t) \\ &= -\frac{2}{3\Omega} \lim_{\eta \rightarrow 0} \int_{-\infty}^{\infty} \rho(\nu) \text{Im} \int_0^{\infty} t dt e^{-i\nu t - \eta t} \\ &= -\frac{2\pi}{3\Omega} \int_{-\infty}^{\infty} \rho(\nu) \frac{d}{d\nu} \delta(\nu) d\nu = \frac{2\pi}{3\Omega} \frac{d\rho}{d\nu} \Big|_{\nu=0}. \end{aligned} \quad (2.14)$$

We shall find it more convenient to rewrite (2.14) in the form:

$$\sigma = \frac{\pi}{3\Omega} \lim_{\nu \rightarrow 0} \frac{1}{\nu} [\rho(\nu) - \rho(-\nu)]. \quad (2.15)$$

The great advantage provided by Eq. (2.15) is that it enables us to calculate  $\sigma$  without evaluating  $\mathfrak{F}(t)$  directly. As was pointed out by other authors,<sup>10-12</sup> simultaneous perturbation expansions of the operators  $\rho_0$  and  $\mathbf{J}(t)$  lead to complicated expressions involving integrations along a path in a complex time-temperature plane. Such a procedure seems to preclude use of the familiar Green's function techniques which have proved so powerful in other problems. If we understand, however, that it is  $\rho$  and not  $\mathfrak{F}$  which is of primary concern, we are free to perform a slightly simpler calculation.

Consider now the function

$$\mathfrak{G}(u) \equiv \text{Tr}\{\rho_0 e^{Hu} \mathbf{J} e^{-Hu} \cdot \mathbf{J}\}. \quad (2.16)$$

Notice that  $\mathfrak{G}$  may be obtained by calculating  $\mathfrak{F}(t)$  for  $t > 0$  and then analytically continuing to  $t = -iu$ . Thus, in principle,  $\mathfrak{G}$  contains as much information about the system as does  $\mathfrak{F}$ . Furthermore, for real values of  $u$  between 0 and  $\beta$ ,  $\mathfrak{G}$  may be evaluated directly by using the propagator techniques devised by Luttinger and Ward.<sup>9</sup> In their graphical notation,  $\mathfrak{G}$  is the sum of all vacuum polarization graphs in which the external vertices occur at 0 and  $u$  and each vertex contains the operator  $\mathbf{J}$ . The standard technique for evaluating  $\mathfrak{G}$  involves computing the Fourier coefficients

$$G_l = \int_0^{\beta} \mathfrak{G}(u) e^{(2\pi i l / \beta) u} du. \quad (2.17)$$

That is, we construct a periodic function with period  $\beta$  whose value is defined by the function  $\mathfrak{G}(u)$  in the interval  $0 < u < \beta$ . The propagator methods of Luttinger and Ward are directly applicable in the evaluation of  $G_l$ . A detailed discussion of these methods is contained in the next section.

The spectral function  $\rho(\nu)$  may be obtained from  $G_l$  in the following way. We insert the complete set of eigenstates of  $H$  ( $|m\rangle$ ,  $|n\rangle$ , etc.) into (2.16) and perform the integration indicated in (2.17). We find

$$\begin{aligned} G_l &= \frac{1}{Z} \sum_{n,m} e^{-\beta(E_n - \mu N_n)} |\langle n | \mathbf{J} | m \rangle|^2 \\ &\quad \times \frac{e^{\beta(E_n - E_m + 2\pi i l / \beta)} - 1}{E_n - E_m + 2\pi i l / \beta}. \end{aligned} \quad (2.18)$$

Next we define a function  $G(\nu)$ , such that

$$G(\nu) = G_l, \quad \nu_l = 2\pi i l / \beta. \quad (2.19)$$

To complete the definition of  $G(\nu)$ , we require that it have a branch cut along the real axis and be analytic everywhere else in the  $\nu$  plane, including  $\infty$  at infinity. According to (2.18), we may obtain such a function by using  $\exp 2\pi i l = 1$  in the numerator of the left-hand side and then identifying  $2\pi i l / \beta \equiv \nu$  in the energy denominator. The discontinuity across the cut is, for

real  $\nu$ ,

$$\begin{aligned} \bar{G}(\nu) &= \frac{1}{2\pi i} \lim_{\eta \rightarrow 0} \{G(\nu + i\eta) - G(\nu - i\eta)\} \\ &= \frac{1}{Z} \sum_{n,m} e^{-\beta(E_n - \mu N_n)} |\langle n | \mathbf{J} | m \rangle|^2 \\ &\quad \times \delta(E_m - E_n - \nu)(1 - e^{-\beta\nu}). \end{aligned} \quad (2.20)$$

By comparing (2.20) with (2.12), we find

$$\rho(\nu) = \frac{\bar{G}(\nu)}{1 - e^{-\beta\nu}}. \quad (2.21)$$

Equation (2.21) completes the connection between the Kubo formula and orthodox many-body perturbation theory.

### III. REDUCED GRAPHS

We turn our attention now to the perturbation expansion of the function  $\bar{G}(\nu)$ . Our aim, as in I and II, is to resum this expansion in such a way that the conductivity  $\sigma$  finally is expressed in the form given by Eq. (1.3). This resummation may be effected via the finite temperature analog of the "reduced graphs" discussed in A. We shall see that the series of reduced graphs yields an expansion of  $\sigma$  in increasing powers of the temperature.

The basic rules for the perturbation expansion of  $G_I$  have been developed in detail by Bloch and De Dominicis.<sup>8</sup> We shall use the propagator version of this formalism devised by Luttinger and Ward.<sup>9</sup> Briefly, the prescription of these authors for the evaluation of  $G_I$  is the following:

1. Draw all possible linked vacuum polarization graphs. Remember that the electrons interact both among themselves and with the static field of the impurities. Remember also that, at this point in the calculation, we are considering a system with a particular configuration of impurities. We shall average over impurity configurations later.

2. With each electron line associate a factor

$$\frac{1}{\beta} S_F(\mathbf{k}, \zeta_l) = -\frac{1}{\beta} \frac{1}{\epsilon_{\mathbf{k}} - \zeta_l}, \quad \zeta_l = \mu + \frac{\pi i}{\beta} (2l + 1). \quad (3.1)$$

Restrict the  $\zeta_l$ 's in such a way that the total  $\zeta$  is conserved at each vertex just as if  $\zeta$  were an energy variable. An impurity interaction<sup>10</sup> transfers no  $\zeta$ . A  $\zeta$  transfer of  $\nu_l$  is to be accounted for at each of the two external vertices.

3. At each internal vertex insert the appropriate interaction potential. At the external vertices insert the current operator  $\mathbf{J}$  and form the scalar product as indicated in Eq. (2.16).

4. For a graph with  $n$  internal interactions and  $c$

closed electron loops, insert a numerical factor

$$(-1)^{n+c}\beta^{n+1}.$$

The factors  $\beta$  arise from the integrations over the variables  $u$  at the vertices. There are  $n+2$  vertices, but one external vertex is fixed at  $u=0$ .

5. Finally, sum over all  $\zeta$ 's, momenta, and spins.

In order to avoid difficulties associated with electron self-energy diagrams, we modify the above rules so as to sum over skeleton graphs. The precise modifications are:

1'. Draw only skeleton graphs, i.e., graphs in which no self-energy parts occur on any electron line. Now we may omit impurity interactions in the diagrams as long as we understand that each electron line represents the exact single-particle propagator calculated in the field of the particular impurity configuration, that we are considering.

2'. With each electron line associate a factor  $1/\beta S_{k,k'}(\zeta_l)$ , where  $S$  is the exact single-particle propagator.  $S$  has the spectral representation<sup>18</sup>

$$S_{k,k'}(\zeta_l) = \int_{-\infty}^{\infty} d\xi \frac{\alpha_{k,k'}(\xi)}{\xi - \zeta_l}, \quad (3.2)$$

where

$$\begin{aligned} \alpha_{k,k'}(\xi) &= \frac{1}{Z} \sum_{n,m} \langle n | a_{\mathbf{k}} | m \rangle \langle m | a_{\mathbf{k}'}^\dagger | n \rangle e^{-\beta(E_n - \mu N_n)} \\ &\quad \times \delta(E_m - E_n - \xi)(e^{\beta(\xi - \mu)} + 1). \end{aligned} \quad (3.3)$$

All other rules remain unchanged except that  $n$  now represents only the number of electron-electron interactions which appear explicitly in a skeleton diagram.

As an example of the application of these rules, let us compute the contribution to  $\rho(\nu)$  from the skeleton graph shown in Fig. 1. We have

$$\begin{aligned} G_I^{(1)} &= -\frac{1}{\beta} \sum_{\text{mom.}, \text{spins}} \sum_{l'} \int d\xi_1 \int d\xi_2 \\ &\quad \times \frac{\alpha(\xi_1)\alpha(\xi_2)}{(\xi_1 - \zeta_{l'}) (\xi_2 - \zeta_{l'} - \nu_l)}. \end{aligned} \quad (3.4)$$

Following Luttinger and Ward,<sup>9</sup> we perform the sum

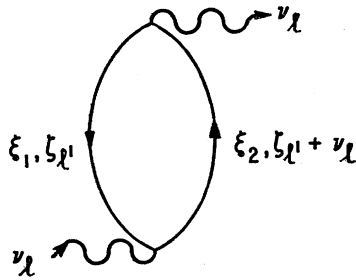


FIG. 1. A simple vacuum polarization graph whose contribution to  $\rho(\nu)$  is computed in the text.

<sup>18</sup> J. M. Luttinger, Phys. Rev. **121**, 942 (1961).

over  $l'$  by using

$$\sum_l F(\xi_l) = (\beta/2\pi i) \oint_{\Gamma} f^-(\omega) F(\omega) d\omega, \quad (3.5)$$

where

$$f^-(\omega) = (e^{\beta(\omega-\mu)} + 1)^{-1}, \quad (3.6)$$

and the contour  $\Gamma$  is drawn in Fig. 2. When, as in (3.4),  $F(\omega)$  contains only simple poles, we may close  $\Gamma$  at infinity to obtain

$$G_l^{(1)} = \sum_{\text{mom., spins}} \int d\xi_1 \int d\xi_2 \mathcal{A}(\xi_1) \mathcal{A}(\xi_2) \times \frac{f^-(\xi_1) - f^-(\xi_2 - \nu_l)}{\xi_2 - \xi_1 - \nu_l}, \quad (3.7)$$

The correct analytic function  $G(\nu)$  is obtained by noting that, because  $\nu_l = 2\pi i l / \beta$ ,  $f^-(\xi - \nu_l) = f^-(\xi)$ . Thus

$$G^{(1)}(\nu) = \sum_{\text{mom., spins}} \int d\xi_1 \int d\xi_2 \mathcal{A}(\xi_1) \mathcal{A}(\xi_2) f^+(\xi_2) f^-(\xi_1) \times \frac{1 - e^{-\beta(\xi_2 - \xi_1)}}{\xi_2 - \xi_1 - \nu}, \quad (3.8)$$

where we have used the identity

$$f^-(\xi_1) - f^-(\xi_2) = f^+(\xi_2) f^-(\xi_1) (1 - e^{-\beta(\xi_2 - \xi_1)}), \quad (3.9)$$

with

$$f^+(\xi) = 1 - f^-(\xi) = (e^{\beta(\xi - \mu)} + 1)^{-1}. \quad (3.10)$$

Finally, from Eqs. (2.20) and (2.21) we have

$$\rho^{(1)}(\nu) = \sum_{\text{mom., spins}} \int d\xi_1 \int d\xi_2 \mathcal{A}(\xi_1) \mathcal{A}(\xi_2) f^+(\xi_2) f^-(\xi_1) \times \delta(\xi_2 - \xi_1 - \nu). \quad (3.11)$$

The definition and evaluation of reduced graphs in the finite temperature problem is somewhat more complicated than it was at zero temperature. The difficulty lies in obtaining the analytic function  $G(\nu)$  from  $G_l$ . If one sets  $\nu_l = \nu$  before summing over  $l'$  in Eq. (3.4), one finds a function with an essential singularity at infinity rather than a branch cut on the real axis. More generally, consider what happens to (2.18) if one sets  $2\pi i l / \beta = \nu$  in (2.17). We must conclude that the techniques of analytic continuation used in A are not applicable in the present problem. We can, however, derive very similar results via a less elegant but analogous procedure.

The contribution to  $G_l$  from any graph  $\gamma$  may be written in the form

$$G_l^{(\gamma)} = \int_{-\infty}^{\infty} d\xi_1 \cdots \int_{-\infty}^{\infty} d\xi_N g(\xi_1, \dots, \xi_N) \times \left\{ \frac{(-1)^{n+\epsilon}}{\beta^L} \sum_{l_1, \dots, l_L} \frac{1}{(\xi_1 - Z_1) \cdots (\xi_N - Z_N)} \right\}, \quad (3.12)$$

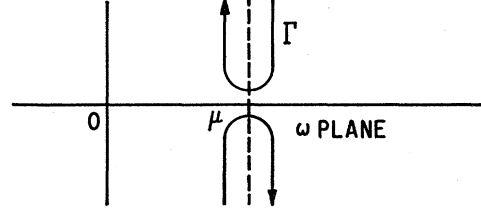


FIG. 2. The contour  $\Gamma$  used in Eq. (3.5).

where  $N$  is the number of internal electron lines and  $L$  is the number of independent closed loops. ( $L = N - n - 1$ ,  $n$  being the number of interactions.) The  $Z$ 's are linear combinations of the  $\xi$ 's and  $\nu_l$  with coefficients  $\pm 1$  or 0.  $g(\xi_1, \dots, \xi_N)$  contains the  $\mathcal{A}$ 's, the explicit interactions, and sums over momenta.

The analysis of  $G_l^{(\gamma)}$  according to A consists of three steps:

1. Hold all the  $\xi$ 's fixed and locate the poles of the quantity in brackets in (3.12). We shall call this quantity  $\{I(\nu)\}$ .
2. Calculate the residues at these poles.
3. The residues generate discontinuities across the cut upon integration over the  $\xi$ 's. Perform these integrations, being careful to sort out contributions from overlapping singularities in such a way that the result resembles a unitarity sum.

First we assert that the result of step 1 must be exactly the same as in the zero-temperature problem. Summation over the  $l$ 's returns us to a time-independent form of the perturbation expansion in which energy denominators occur. The poles arise at the values of  $\nu$  where certain of these energy denominators vanish. The point here is that just the same energy denominators must occur in the finite-temperature theory as in the zero-temperature theory. To see this, we may return to the explicitly time (temperature) dependent form of the expansion. That is, insert

$$\frac{1}{\beta} \sum_l \int_{-\infty}^{\infty} d\xi \frac{\mathcal{A}_{k,k'}(\xi)}{\xi - \zeta_l} e^{-\zeta_l u} = \int_{-\infty}^{\infty} d\xi \mathcal{A}_{k,k'}(\xi) e^{-\xi u} f^+(\xi), \quad \beta > u > 0; \\ = - \int_{-\infty}^{\infty} d\xi \mathcal{A}_{k,k'}(\xi) e^{-\xi u} f^-(\xi), \quad -\beta < u < 0, \quad (3.13)$$

for each electron line and

$$\delta_{\zeta_1 + \zeta_2, \zeta_3 + \zeta_4} = \frac{1}{\beta} \int_0^\beta \exp \left\{ \frac{2\pi i u}{\beta} (l_1 + l_2 - l_3 - l_4) \right\} du \quad (3.14)$$

at each vertex. The resulting expression has precisely the same form as the time-ordered product which occurs in the zero-temperature theory except for the

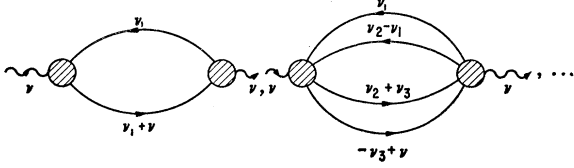


FIG. 3. The reduced graphs associated with the vacuum polarization function.

presence of the Fermi functions  $f^\pm(\xi)$  and the fact that the range of integration over (real)  $u$  is finite. It is obvious, however, that the  $u$  integrations will bring down the same energy denominators as do the  $t$  integrations. Furthermore, we may sum over all time orders which do not change the particle- or hole-like nature of any line without changing the Fermi functions. According to the discussion in A, the denominators which remain after this summation yield true poles in  $I$ .

We now repeat the prescription given in A for location of a pole in the function  $I(\nu)$ . We look for an intermediate state such that, if all the electron lines in this state were broken, the graph would separate into just two pieces. Each of these pieces must be connected and each must contain one of the external vertices. A pole occurs at that value of  $\nu$  for which the energy denominator associated with this state vanishes. A graph in which only this intermediate state and the external lines are exhibited has been called a "reduced" graph. The reduced graphs relevant to  $I(\nu)$  are all of the form shown in Fig. 3.

Our second step is to compute the residue of the pole associated with any one of these reduced graphs. For convenience in performing this calculation we introduce a few minor changes in notation. Let us now measure  $\xi$

from the chemical potential  $\mu$ ; i.e.,

$$\xi = \xi' + \mu. \quad (3.15)$$

Usually we shall omit the primes on the new  $\xi$ 's. Also let us consider the propagator  $S$  simply as a function of  $\nu_i = 2\pi i l / \beta$ . Thus

$$S_{k,k'}(\nu_i) = \int d\xi \frac{Q_{k,k'}(\xi)}{\xi - \pi i / \beta - \nu_i}. \quad (3.16)$$

Conservation of  $\zeta$  at each vertex becomes conservation of  $\nu$ , the advantage of the form (3.16) being that  $\nu_i + \nu_m = \nu_{i+m}$ . To perform sums over  $\nu_i$  we shall use

$$\frac{1}{\beta} \sum_i A(\nu_i) = \frac{1}{2\pi i} \oint_C d\nu h(\nu) A(\nu), \quad (3.17)$$

where

$$h(\nu) = (e^{\beta\nu} - 1)^{-1} \quad (3.18)$$

and  $A$  is any function of  $\nu$ . The contour  $C$  encloses all the poles of  $h$  and none of those of  $A$ . Note that

$$h(\xi - \pi i / \beta) = -f^-(\xi). \quad (3.19)$$

Finally, we often shall write  $\nu_1, \nu_2, \dots$  instead of  $\nu_{i_1}, \nu_{i_2}, \dots$ .

Now label the lines in any reduced graph in the manner suggested by the labeling in Fig. 3. That is, the lines running from right to left (hole lines) are labeled  $\nu_1, \nu_2 - \nu_1, \nu_3 - \nu_2, \dots, \nu_p - \nu_{p-1}$ , where  $p$  is the number of intermediate particle-hole pairs. The lines running from left to right (particle lines) are labeled  $\nu_p + \nu_{p+1}, \nu_{p+2} - \nu_{p+1}, \dots, \nu - \nu_{2p-1}$ . This labeling automatically conserves  $\nu$  in the diagram. The function  $I$  may be written in the form

$$I(\nu) = \frac{1}{\beta^{2p-1}} \sum_{\nu_1, \dots, \nu_{2p-1}} \frac{I_{2p}(\nu_1, \dots, \nu_{2p-1}, \nu)}{(\xi_1 - i\pi/\beta - \nu_1) \cdots (\xi_{2p} - i\pi/\beta + \nu_{2p-1} - \nu)}, \quad (3.20)$$

where  $I_{2p}$  contains all the remaining sums associated with lines not drawn explicitly in the reduced diagram.  $I_{2p}$  must be chosen to be an analytic function of the  $\nu$ 's having only poles and no singularities at infinity.

Our procedure here is very similar to that of A. We suppose that all sums have been performed except that over  $\nu_1$  and write

$$I(\nu) = \frac{1}{\beta} \sum_{\nu_1} \frac{1}{\xi_1 - i\pi/\beta - \nu_1} I_1(\nu_1, \nu) \\ = \frac{1}{2\pi i} \oint_C d\nu_1 h(\nu_1) \frac{I_1(\nu_1, \nu)}{\xi_1 - i\pi/\beta - \nu_1}, \quad (3.21)$$

where  $I_1$  satisfies the same condition of analyticity as  $I_{2p}$ . Then select one pole of  $I_1$  in the complex  $\nu_1$  plane. That is, write

$$I_1(\nu_1, \nu) = \frac{R_1(\nu)}{P_1(\nu) - \nu_1} + J_1(\nu_1, \nu), \quad (3.22)$$

where  $J_1$  is analytic in the neighborhood of  $\nu_1 = P_1$ . The contribution of this part of  $I_1$  to  $I$  is

$$I_S(\nu) = \frac{1}{2\pi i} \oint_C d\nu_1 h(\nu_1) \frac{R_1(\nu)}{(\xi_1 - i\pi/\beta - \nu_1)(P_1 - \nu_1)} \\ = \frac{R_1}{P_1 - \xi_1 + i\pi/\beta} [h(\xi_1 - i\pi/\beta) - h(P_1)]. \quad (3.23)$$

If we make the *ansatz*

$$P_1 = E_1 - i\pi/\beta - \nu, \quad (3.24)$$

then

$$I_S(\nu) = -\frac{R_1(\nu)}{E_1 - \xi_1 - \nu} f^+(E_1) f^-(\xi_1) (1 - e^{-\beta(E_1 - \xi_1)}), \quad (3.25)$$

where we have used Eqs. (3.9), (3.10), and (3.19).

In order to find  $R_1$  and  $E_1$ , we simply repeat the above procedure selecting the pole associated with the second

line in the reduced graph. That is, we write

$$I_1(\nu_1, \nu) = \frac{1}{\beta} \sum_{\nu_2} \frac{1}{\xi_2 - i\pi/\beta - \nu_2 + \nu_1} I_2(\nu_1, \nu_2, \nu). \quad (3.26)$$

We isolate a pole of  $I_2$  in the  $\nu_2$  plane,

$$I_2(\nu_1, \nu_2, \nu) = \frac{R_2}{P_2 - \nu_2} + J_2(\nu_1, \nu_2, \nu), \quad (3.27)$$

and make the *ansatz*

$$P_2 = E_2 - i\pi/\beta - \nu. \quad (3.28)$$

The resulting singular part of  $I_1$  is

$$\begin{aligned} I_{1S} &= \frac{1}{2\pi i} \oint_C d\nu_2 h(\nu_2) \\ &\quad \times \frac{R_2}{(\xi_2 - i\pi/\beta + \nu_1 - \nu_2)(E_2 - i\pi/\beta - \nu - \nu_2)} \\ &= \frac{R_2}{E_2 - \xi_2 - \nu_1 - \nu} \\ &\quad \times f^-(\xi_2) f^+(E_2) (1 - e^{-\beta(E_2 - \xi_2)}). \end{aligned} \quad (3.29)$$

Then

$$P_1 = E_1 - i\pi/\beta - \nu = E_2 - \xi_2 - \nu \quad (3.30)$$

implies

$$E_1 = E_2 - \xi_2 + i\pi/\beta, \quad (3.31)$$

which justifies the *ansatz* (3.24) on the basis of (3.28). For the residue we have, using (3.31),

$$R_1(\nu) = -R_2(\nu) \frac{f^-(\xi_2) f^+(E_2)}{f^+(E_1)}, \quad (3.32)$$

where it is understood that  $R_2$  here is to be evaluated at  $\nu_1 = P_1$ . The remaining singular part of  $I$  is

$$I_S(\nu) = \frac{R_2(\nu)}{E_1 - \xi_1 - \nu} f^+(E_2) f^-(\xi_2) f^-(\xi_1) \times (1 - e^{-\beta(E_1 - \xi_1)}). \quad (3.33)$$

The above procedure must be repeated for each of the hole lines  $1 \leq r \leq p-1$ , according to the rules

$$P_{r+1} \equiv E_{r+1} - i\pi/\beta - \nu; \quad (3.34)$$

$$E_r = E_{r+1} - \xi_{r+1} + i\pi/\beta; \quad (3.35)$$

$$R_r = -R_{r+1} \frac{f^-(\xi_{r+1}) f^+(E_{r+1})}{f^+(E_r)}. \quad (3.36)$$

Beginning with the first particle line, however, we change the *ansatz* (3.34) to

$$P_{r+1} = E_{r+1} - i\pi/\beta + \nu, \quad p \leq r \leq 2p. \quad (3.37)$$

This leads to

$$E_p = -E_{p+1} + \xi_{p+1} + i\pi/\beta \quad (3.38)$$

and

$$R_p = -R_{p+1} \frac{f^+(\xi_{p+1}) f^-(E_{p+1})}{f^+(E_p)}. \quad (3.39)$$

For  $r \geq p+1$ , the rules for iteration are

$$E_r = E_{r+1} - \xi_{r+1} + i\pi/\beta; \quad (3.40)$$

and

$$R_r = R_{r+1} \frac{f^-(E_{r+1}) f^+(\xi_{r+1})}{f^-(E_r)}. \quad (3.41)$$

Finally, at  $r = 2p-1$ , we have [from Eq. (3.20)]

$$P_{2p-1} = E_{2p-1} - i\pi/\beta + \nu = -\xi_{2p} + i\pi/\beta + \nu; \quad (3.42)$$

thus,

$$E_{2p-1} = -\xi_{2p} + 2i\pi/\beta. \quad (3.43)$$

Working backwards, using (3.43), (3.40), (3.38), and (3.35), we find

$$E_1 = \xi_{2p} + \dots + \xi_{p+1} - \xi_p - \dots - \xi_2. \quad (3.44)$$

Similarly, for the residues, we have

$$R_{2p-1} = -I_{2p}, \quad (3.45)$$

where it is understood that  $I_{2p}$  is here to be evaluated at the values  $\nu_r = P_r$ . From Eqs. (3.34), (3.35), (3.37), and (3.40) we see that this last condition implies

$$\nu_r - \nu_{r-1} = E_r - E_{r-1} = \xi_r - i\pi/\beta, \quad r \neq p \text{ or } 2p-1. \quad (3.46)$$

For  $r = p$  we have, from Eq. (3.38),

$$\nu_p + \nu_{p+1} = E_p + E_{p+1} - 2\pi i/\beta = \xi_{p+1} - i\pi/\beta; \quad (3.47)$$

and, for  $r = 2p-1$ , Eq. (3.42) yields

$$\nu_{2p-1} = P_{2p-1} = E_{2p-1} - i\pi/\beta + \nu = -\xi_{2p} + i\pi/\beta + \nu. \quad (3.48)$$

In the notation of (3.12), the last three equations imply

$$\xi_r - Z_r = 0 \quad (3.49)$$

for all lines in the reduced diagram. Equation (3.49) is exactly the first of the two Landau equations discussed in A. By iterating Eqs. (3.36), (3.39), and (3.41) starting from (3.45), we find

$$R_1(\nu) = \frac{(-1)^{p+1}}{f^+(E_1)} f^-(\xi_2) \dots f^-(\xi_p) f^+(\xi_{p+1}) \dots \times f^+(\xi_{2p}) I_{2p}(\nu_r = P_r). \quad (3.50)$$

Thus, the complete expression for the singular part of  $I(\nu)$  is

$$\begin{aligned} I_S(\nu) &= (-1)^{p+1} \frac{(1 - e^{-\beta(\xi_{2p} + \dots + \xi_{p+1} - \xi_p - \dots - \xi_1 - \nu)})}{\xi_{2p} + \dots + \xi_{p+1} - \xi_p - \dots - \xi_1 - \nu} \\ &\quad \times f^+(\xi_{2p}) \dots f^+(\xi_{p+1}) f^-(\xi_p) \dots f^-(\xi_1) \\ &\quad \times I_{2p}(\nu_r = P_r). \end{aligned} \quad (3.51)$$

Notice that the restrictions on the  $\xi$ 's imposed by the second Landau equation are included in (3.51) via the Fermi factors  $f^\pm(\xi)$  associated with each of the

lines. The entire right-hand side of (3.51) is a simple pole associated with the energy denominator for the intermediate state described by a reduced graph. This completes the second step of the analysis.

The third step in the analysis of reduced graphs is the integration over the  $\xi$ 's to find the discontinuity across the branch cut. The only difficulty here arises when, for some values of the  $\xi$ 's, one or more poles in  $I_{2p}(\nu)$  happen to coincide with the explicit pole in (3.51). This situation must be treated in exactly the same way as in A; and we shall not repeat those arguments here. The result is the following. The function  $I_{2p}(\nu)$  consists of two parts, say  $M_1(\nu)$  and  $M_2(\nu)$ , associated with the two shaded circles in each of the graphs of Fig. 3. For the contribution to the discontinuity  $\bar{G}$  from any reduced graph we must write an expression of the form:

$$\begin{aligned} \bar{G}^{(p)}(\nu) = & \int_{-\infty}^{\infty} d\xi_1 \cdots \int_{-\infty}^{\infty} d\xi_N g(\xi_1, \dots, \xi_N) \\ & \times \lim_{\eta \rightarrow 0} [M_1(\nu - i\eta) M_2(\nu + i\eta)] f^+(\xi_{2p}) \cdots \\ & \times f^+(\xi_{p+1}) f^-(\xi_p) \cdots f^-(\xi_1) \\ & \times \delta(\xi_{2p} + \cdots + \xi_{p+1} - \xi_p - \cdots - \xi_1 - \nu) \\ & \times (-1)^{p+1} (1 - e^{-\beta\nu}). \end{aligned} \quad (3.52)$$

We may sum over all reduced graphs of order  $2p$  by summing over all possible combinations of  $M_1$  and  $M_2$ . Here we must be careful to construct only skeleton diagrams. Then it is simpler to write the quantity in square brackets in (3.52) as  $[M_1 M_2^*]$  with the understanding that the  $M$ 's are functions of the  $\xi$ 's. As pointed out in A, this result is very similar to a unitarity sum.

#### IV. EVALUATION OF THE CONDUCTIVITY

The mathematical techniques discussed in the last section are now to be applied to the evaluation of the conductivity. First use the definition of  $\rho$  in Eq. (2.21) and rewrite (3.52) in the form

$$\begin{aligned} \rho^{(p)}(\nu) = & (-1)^{p+1} \int_{-\infty}^{\infty} d\xi_1 \cdots \int_{-\infty}^{\infty} d\xi_{2p} \\ & \times \delta(\xi_{2p} + \cdots + \xi_{p+1} - \xi_p - \cdots - \xi_1 - \nu) \\ & \times f^+(\xi_{2p}) \cdots f^+(\xi_{p+1}) f^-(\xi_p) \cdots f^-(\xi_1) \\ & \times \left[ \sum_{\gamma} \sum_{\text{mom., spins}} \mathbf{\Lambda}_1^{(p)} \cdot \mathbf{\Lambda}_2^{(p)*} \mathcal{Q}(\xi_1) \cdots \mathcal{Q}(\xi_{2p}) \right]. \end{aligned} \quad (4.1)$$

The vertex functions  $\mathbf{\Lambda}$  now contain all the interactions,  $\xi$  integrations, and momentum sums implied by the shaded circles in the reduced diagrams. Note that the spectral functions  $\mathcal{Q}$  associated with the  $2p$  internal lines of the reduced graph are written explicitly. This accounts for all the factors previously included in the function  $g(\xi_1, \dots, \xi_N)$ . It must be understood that the

$\mathbf{\Lambda}$ 's are functions of  $\xi_1, \dots, \xi_{2p}$  and also of the momenta. Momentum subscripts have been suppressed throughout. The sum over  $\gamma$  means that we are to sum over all combinations of vertex diagrams  $\mathbf{\Lambda}_1^{(p)} \cdot \mathbf{\Lambda}_2^{(p)*}$  in such a way as to form all possible reduced skeleton diagrams of order  $p$ .

Next we must form the function  $\rho^{(p)}(-\nu)$  in order to evaluate  $\sigma$  as given by Eq. (2.15). To do this, notice that the quantity in square brackets in Eq. (4.1) is symmetric under the exchange of variables  $\xi_1 \leftrightarrow \xi_{p+1}, \dots, \xi_p \leftrightarrow \xi_{2p}$ . That is, we exchange the particle and hole variables. The symmetry follows simply from the structure of the diagrams. By using this symmetry, we may write<sup>18a</sup>

$$\begin{aligned} \rho^{(p)}(-\nu) = & (-1)^{p+1} \int_{-\infty}^{\infty} d\xi_1 \cdots \int_{-\infty}^{\infty} d\xi_{2p} \\ & \times \delta(\xi_{2p} + \cdots - \xi_1 - \nu) f^-(\xi_{2p}) \cdots \\ & \times f^-(\xi_{p+1}) f^+(\xi_p) \cdots f^+(\xi_1) \\ & \times \left[ \sum_{\gamma} \sum_{\text{mom., spins}} \mathbf{\Lambda}_1^{(p)} \cdot \mathbf{\Lambda}_2^{(p)*} \mathcal{Q}(\xi_1) \cdots \mathcal{Q}(\xi_{2p}) \right]. \end{aligned} \quad (4.2)$$

The resulting contribution to  $\sigma$  according to (2.15) contains a factor:

$$\begin{aligned} & f^+(\xi_{2p}) \cdots f^+(\xi_{p+1}) f^-(\xi_p) \cdots f^-(\xi_1) \\ & - f^-(\xi_{2p}) \cdots f^-(\xi_{p+1}) f^+(\xi_p) \cdots f^+(\xi_1). \end{aligned} \quad (4.3)$$

If we use the identity

$$f^+(\xi) = e^{\beta(\xi - \mu)} f^-(\xi), \quad (4.4)$$

we may write the expression (4.3) in the form

$$\begin{aligned} & f^+(\xi_{2p}) \cdots f^+(\xi_{p+1}) f^-(\xi_p) \cdots f^-(\xi_1) \\ & \times \left[ 1 - \exp\{-\beta(\xi_{2p} + \cdots + \xi_{p+1} - \xi_p - \cdots - \xi_1)\} \right]. \end{aligned} \quad (4.5)$$

Then

$$\begin{aligned} \sigma = & \frac{\pi}{3\Omega} \sum_p (-1)^{p+1} \lim_{\nu \rightarrow 0} \frac{1}{\nu} \int_{-\infty}^{\infty} d\xi_1 \cdots \int_{-\infty}^{\infty} d\xi_{2p} \\ & \times \delta(\xi_{2p} + \cdots - \xi_1 - \nu) f^+(\xi_{2p}) \cdots \\ & \times f^+(\xi_{p+1}) f^-(\xi_p) \cdots f^-(\xi_1) (1 - e^{-\beta\nu}) \\ & \times \left[ \sum_{\gamma} \sum_{\text{mom., spins}} \mathbf{\Lambda}_1^{(p)} \cdot \mathbf{\Lambda}_2^{(p)*} \mathcal{Q}(\xi_1) \cdots \mathcal{Q}(\xi_{2p}) \right] \\ = & \frac{\beta\pi}{3\Omega} \sum_p (-1)^{p+1} \int_{-\infty}^{\infty} d\xi_1 \cdots \int_{-\infty}^{\infty} d\xi_{2p} \\ & \times \delta(\xi_{2p} + \cdots - \xi_1) f^+(\xi_{2p}) \cdots f^-(\xi_1) \\ & \times \left[ \sum_{\gamma} \sum_{\text{mom., spins}} \mathbf{\Lambda}_1^{(p)} \cdot \mathbf{\Lambda}_2^{(p)*} \mathcal{Q}(\xi_1) \cdots \mathcal{Q}(\xi_{2p}) \right]. \end{aligned} \quad (4.6)$$

<sup>18a</sup> Note added in proof. It follows from Eq. (2.12) that

$$\rho(-\nu) = e^{-\beta\nu} \rho(\nu);$$

thus, from Eq. (2.15)

$$\sigma = (\pi\beta/3\Omega)\rho(0),$$

which is equivalent to the final form of Eq. (4.6).

The temperature dependence of the  $p$ th term in the conductivity as given by (4.6) may be determined by standard techniques. The delta function and the Fermi factors restrict the  $\xi$ 's to a region of order  $k_B T$  about the chemical potential  $\mu$ . For sufficiently small temperatures, we may evaluate (4.6) by expanding the quantity in square brackets as a power series about  $\xi = \mu$ . If we take only the leading term in this expansion we find a factor

$$\beta \int_{-\infty}^{\infty} d\xi_1 \cdots \int_{-\infty}^{\infty} d\xi_{2p} \delta(\xi_{2p} + \cdots - \xi_1) f^+(\xi_{2p}) \cdots f^-(\xi_1) = \beta^{2-2p} \times \text{const.} \quad (4.7)$$

It follows that the set of reduced graphs generates an expansion of the conductivity in increasing even powers of the temperature.

In order to take the zero temperature limit of (4.6) we need consider only the term for which  $p=1$ . This is

$$\begin{aligned} \sigma^{(1)} &= \frac{\beta\pi}{3\Omega} \int_{-\infty}^{\infty} d\xi f^+(\xi) f^-(\xi) \\ &\quad \times \left[ \sum_{\gamma} \sum_{\text{mom., spins}} \mathbf{\Lambda}_1^{(1)} \cdot \mathbf{\Lambda}_2^{(1)*} \mathcal{Q}(\xi) \mathcal{Q}(\xi) \right] \\ &= -\frac{\pi}{3\Omega} \int_{-\infty}^{\infty} \frac{df^-}{d\xi} d\xi \\ &\quad \times \left[ \sum_{\text{mom., spins}} \mathbf{\Lambda}^{(1)} \cdot \mathbf{\Lambda}^{(1)*} \mathcal{Q}(\xi) \mathcal{Q}(\xi) \right]. \quad (4.8) \end{aligned}$$

As  $T \rightarrow 0$ , (4.8) becomes

$$\sigma(T=0) = \frac{\pi}{3\Omega} \lim_{T \rightarrow 0} \left[ \sum_{\text{mom., spins}} \mathbf{\Lambda}^{(1)} \cdot \mathbf{\Lambda}^{(1)*} \mathcal{Q}(\mu) \mathcal{Q}(\mu) \right], \quad (4.9)$$

which is precisely the same as Eq. (2.12) in II. Notice the following points. For this lowest order reduced graph ( $p=1$ ) we have summed over graphs simply by replacing  $\mathbf{\Lambda}_1^{(1)}$  and  $\mathbf{\Lambda}_2^{(1)}$  by the sum of all vertex diagrams, indicated by the symbol  $\mathbf{\Lambda}^{(1)}$  as in II. This cannot be done for higher order graphs without constructing diagrams which are not skeleton-like. Also notice that the functions  $\mathbf{\Lambda}^{(1)}$  and  $\mathcal{Q}$  are still temperature dependent through the  $\beta$  and  $\mu$  which appear in the definition of  $\zeta_l$ . As discussed by Luttinger and Ward, however, in their zero-temperature limits these functions become the same as those used previously. This completes the proof that the expression for the conductivity given in II is the exact zero-temperature limit of a complete statistical formulation of transport theory.

## V. CORRECTIONS OF ORDER $T^2$

The final section of this paper is devoted to a discussion of the lowest order finite temperature corrections to Eq. (4.9). As pointed out above, these corrections are of order  $T^2$ . They arise in two places. First, there

are terms of order  $T^2$  occurring in the lowest order reduced graph as given by Eq. (4.8). Second, there is a contribution from the reduced graph of order  $p=2$ .

We consider first the term  $\sigma^{(1)}$  as given by Eq. (4.8). The final expression on the right-hand side of this equation has a form very similar to the Greenwood-Peierls formula<sup>19</sup> used as a starting point by Edwards<sup>4</sup> and by Chester and Thellung<sup>5</sup> in their evaluations of the conductivity of a system of independent electrons. In fact, Eq. (4.8) represents the generalization of the Greenwood-Peierls formula to a system of noninteracting quasi-particles. We may interpret the various factors as follows. The factor  $\beta f^+(\xi) f^-(\xi)$  tells us that the conductivity is determined predominantly only by those particles whose energies  $\xi$  lie within  $k_B T$  of the Fermi surface. The vertex function  $\mathbf{\Lambda}^{(1)}$  is, apart from the normalization factor discussed in II, the current ( $e/m \times$  group velocity) of a single quasi-particle. To prove this, note that we may insert the current operator into any internal electron line by using the relationship

$$S_F(\mathbf{k}, \zeta_l) (ek_i/m) S_F(\mathbf{k}, \zeta_l) = -e(\partial/\partial k_i) S_F(\mathbf{k}, \zeta_l). \quad (5.1)$$

The Ward identity,

$$\mathbf{\Lambda}_i^{(1)}(\mathbf{k}, \zeta_l) = (e/m)k_i - e(\partial/\partial k_i) \Sigma'(\mathbf{k}, \zeta_l), \quad (5.2)$$

follows immediately.  $\Sigma'$  is the usual self-energy function, computed here in the absence of impurities.  $\mathbf{\Lambda}^{(1)}$  is now a function of the temperature via the electron-electron interactions. That is, the propagation of a quasi-particle is affected by the thermal fluctuations of the background medium in which it moves.

The spectral functions  $\mathcal{Q}(\xi)$  have the effect of constraining the particles to lie on or near the energy shell; i.e., they insist that the energy  $\xi$  and the momentum very nearly satisfy the dispersion relation for real quasi-particles. To be more specific, let us consider the function  $\langle \mathcal{Q}_k(\xi) \rangle$ , where the angular brackets denote the average over configurations of impurities. We construct  $\langle \mathcal{Q} \rangle$  from the average single-particle propagator [Eq. (3.2)], which we may write in the form

$$\langle S_{\mathbf{k}, \mathbf{k}'}(\zeta_l) \rangle_{\text{av}} = \langle S(\mathbf{k}, \zeta_l) \rangle \delta_{\mathbf{k}, \mathbf{k}'} = \frac{\delta_{\mathbf{k}, \mathbf{k}'}}{\epsilon_{\mathbf{k}} - \zeta_l - \Sigma(\mathbf{k}, \zeta_l)}. \quad (5.3)$$

Analytic continuation to real values of  $\zeta_l$  yields (see Luttinger<sup>18</sup>)

$$\lim_{\eta \rightarrow 0} \Sigma(\mathbf{k}, \xi \pm i\eta) = \Delta(\mathbf{k}, \xi) \pm i\Gamma(\mathbf{k}, \xi); \quad (5.4)$$

and

$$\begin{aligned} \langle \mathcal{Q}_k(\xi) \rangle &= (1/2\pi i) \lim_{\eta \rightarrow 0} [\langle S(\mathbf{k}, \xi + i\eta) \rangle - \langle S(\mathbf{k}, \xi - i\eta) \rangle] \\ &= \frac{1}{\pi} \frac{\Gamma(\mathbf{k}, \xi)}{[\epsilon_{\mathbf{k}} - \xi - \Delta(\mathbf{k}, \xi)]^2 + \Gamma(\mathbf{k}, \xi)^2}. \quad (5.5) \end{aligned}$$

Thus, if  $\Gamma$  is small and slowly varying, the function  $\langle \mathcal{Q} \rangle$  looks like a slightly broadened delta function

<sup>19</sup> D. A. Greenwood, Proc. Phys. Soc. (London) **71**, 585 (1958).

peaked near

$$\epsilon_{\mathbf{k}} - \xi - \Delta(\mathbf{k}, \xi) = 0. \quad (5.6)$$

The width of this peak  $\Gamma$  is a measure of the uncertainty in the quasi-particle energy, and is related to the rate of relaxation relevant to the resistivity. A more complete discussion of these points may be found in papers I and II.

It is convenient to decompose  $\Gamma$  into two parts:

$$\Gamma(\mathbf{k}, \xi) = \Gamma_e(\mathbf{k}, \xi) + \Gamma_{\text{imp.}}(\mathbf{k}, \xi), \quad (5.6)$$

where  $\Gamma_e$  is that part of  $\Gamma$  which arises solely from electron-electron interactions. All the impurity effects are contained in  $\Gamma_{\text{imp.}}$ . In the zero-temperature problem, as discussed in A and by Luttinger,<sup>18</sup>  $\Gamma_e$  behaves like  $(\xi - \mu)^2$  near the Fermi surface. That is low-lying quasi-particle excitations are nearly stable. For the conductivity at absolute zero temperature we needed only the value of  $\Gamma$  at  $\xi = \mu$ ; thus  $\Gamma_e$  did not contribute. At finite temperature, however,  $(\xi - \mu)^2$  is of order  $(k_B T)^2$ , and must be retained in the present calculation. Furthermore,  $\Gamma_e(\mathbf{k}, \mu)$  is itself of the order  $(k_B T)^2$ . We conclude that the quasi-particles relevant to the conductivity as given by Eq. (4.8) have an intrinsic decay rate, independent of the impurities, of order  $T^2$ . On the other hand, because the total current is conserved in electron-electron collisions,  $\Gamma_e$  cannot contribute to the relaxation rate which occurs in the final formula for the conductivity. There must then be an exact cancellation of this  $T^2$  term.

In order to find this cancellation without all of the complications involved in the complete average over impurity configurations, let us simply replace the  $\alpha$ 's which occur in Eq. (4.8) by  $\langle \alpha \rangle$ 's. That is, we examine the terms of order  $T^2$  occurring in the expression

$$\bar{\sigma}^{(1)} = \frac{2\pi\beta}{3\Omega} \int_{-\infty}^{\infty} d\xi f^+(\xi) f^-(\xi) \times \sum_{\mathbf{k}} |\Lambda^{(1)}(\mathbf{k}, \xi)|^2 \langle \alpha_{\mathbf{k}}(\xi) \rangle^2. \quad (5.7)$$

In principle, of course, (5.7) omits the cross terms in the impurity average which, in the zeroth order calculation, give rise to the "scattering-in" part of the relaxation rate. It is a straightforward but tedious exercise to include these terms correctly in the following analysis. In fact, we shall see that the following  $T^2$  corrections remain finite in the limit of zero impurity concentration; thus there is no real approximation involved here. As in all previous work, we shall systematically omit all contributions to the conductivity except those which behave like  $n_i^{-1}$ .

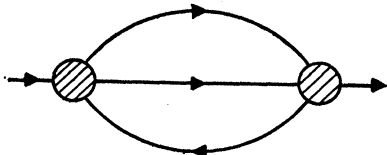


FIG. 4. The lowest order reduced graph associated with the electron self-energy function.

As long as  $\Lambda$  and  $\Gamma$  are slowly varying functions of  $\mathbf{k}$ , we may write

$$\langle \alpha_{\mathbf{k}}(\xi) \rangle^2 = [1/2\pi\Gamma(\mathbf{k}, \xi)] \delta[\epsilon_{\mathbf{k}} - \xi - \Delta(\mathbf{k}, \xi)]. \quad (5.8)$$

The corrections to Eq. (5.8) are of order  $\Gamma$  and may be neglected to lowest order in  $n_i$ . Now to order  $T^2$  we may write

$$\frac{1}{\Gamma(\mathbf{k}, \xi)} = \frac{1}{\Gamma_{\text{imp.}} + \Gamma_e} \cong \frac{1}{\Gamma_{\text{imp.}}} - \frac{\Gamma_e}{\Gamma_{\text{imp.}}^2} + \dots \quad (5.9)$$

Thus we consider a  $T^2$  correction in (5.7) of the form

$$-\frac{2\pi\beta}{3\Omega} \int_{-\infty}^{\infty} d\xi f^+(\xi) f^-(\xi) \times \left[ \sum_{\mathbf{k}} |\Lambda^{(1)}(\mathbf{k}, \xi)|^2 \frac{\Gamma_e(\mathbf{k}, \xi)}{2\pi\Gamma_{\text{imp.}}^2} \delta[\epsilon_{\mathbf{k}} - \xi - \Delta(\mathbf{k}, \xi)] \right]. \quad (5.10)$$

At this point we must evaluate  $\Gamma_e(\mathbf{k}, \xi)$  via the same sort of analysis as that used in Sec. III of this paper. Only the lowest order reduced graph, drawn in Fig. 4, contributes to order  $T^2$  in (5.10). The contribution of this graph to  $\Gamma_e$  turns out to be

$$\Gamma_e(\mathbf{k}, \xi) = \frac{\pi}{f^+(\xi)} \int \int \int d\xi_1 d\xi_2 d\xi_3 \times \delta(\xi_1 + \xi_2 - \xi_3 - \xi) f^+(\xi_1) f^+(\xi_2) f^-(\xi_3) \times \sum_{\text{mom., spins}} |T|^2 \alpha(\xi_1) \alpha(\xi_2) \alpha(\xi_3), \quad (5.11)$$

where  $T$  represents the part of the diagram indicated by the small shaded circle in the figure. Notice that  $T$  is just the scattering amplitude for two quasi-particles.

The remainder of the quantity in square brackets in (5.10) now may be evaluated to zeroth order in the temperature and at  $\xi = \mu$ . Thus, we may write

$$\lim_{T \rightarrow 0} \frac{1}{2\pi\Gamma_{\text{imp.}}^2} \delta[\epsilon_{\mathbf{k}} - \mu - \Delta(\mathbf{k}, \mu)] = \frac{1}{\pi^2} \frac{\Gamma_{\text{imp.}}}{[(\epsilon_{\mathbf{k}} - \mu - \Delta)^2 + \Gamma_{\text{imp.}}^2]^2} = \frac{1}{\pi} |\langle S(\mathbf{k}, \mu) \rangle|^2 \langle \alpha_{\mathbf{k}}(\mu) \rangle. \quad (5.12)$$

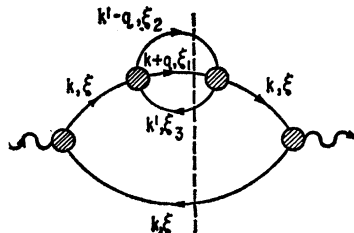


FIG. 5. A graphical representation of the expression (5.13).

Inserting (5.11) and (5.12) into (5.10), we find to order  $T^2$

$$\begin{aligned}
 & -\frac{\pi\beta}{3\Omega} \int \int \int \int d\xi_1 d\xi_2 d\xi_3 d\xi \\
 & \quad \times \delta(\xi_1 + \xi_2 - \xi_3 - \xi) f^+(\xi_1) f^+(\xi_2) f^-(\xi_3) f^-(\xi) \\
 & \quad \times \lim_{T \rightarrow 0} \sum_{\text{mom., spins}} |\mathbf{\Lambda}^{(1)}(\mathbf{k}, \mu) \langle S(\mathbf{k}, \mu) \rangle \mathbf{T}|^2 \\
 & \quad \times \langle \mathcal{G}_{\mathbf{k}}(\mu) \rangle \langle \mathcal{G}_{\mathbf{k}+\mathbf{q}}(\mu) \rangle \langle \mathcal{G}_{\mathbf{k}'}(\mu) \rangle \langle \mathcal{G}_{\mathbf{k}'-\mathbf{q}}(\mu) \rangle. \quad (5.13)
 \end{aligned}$$

Here we have again averaged over impurity configurations simply by replacing the  $\mathcal{G}$ 's in (5.11) by  $\langle \mathcal{G} \rangle$ 's. The expression (5.13) may be associated with the diagram drawn in Fig. 5. In (5.13) this diagram has been evaluated as if it were a reduced graph of order  $p=2$ , the intermediate state consisting of those lines which are cut by the dashed line in the figure. That is, we combine the quantities  $\mathbf{\Lambda}^{(1)}(\mathbf{k}, \mu) \langle S(\mathbf{k}, \mu) \rangle \mathbf{T}$  into a single vertex and relabel this  $\mathbf{\Lambda}^{(2)}$ . Notice that we might just as well have drawn Fig. 5 with the self-energy part inserted into the hole line rather than the particle line. To do this, simply rewrite Eq. (5.11) for  $\Gamma_e$  by using the identity

$$\frac{f^+(\xi_1) f^+(\xi_2) f^-(\xi_3)}{f^+(\xi_1 + \xi_2 - \xi_3)} = \frac{f^-(\xi_1) f^-(\xi_2) f^+(\xi_3)}{f^-(\xi_1 + \xi_2 - \xi_3)}. \quad (5.14)$$

It is convenient to associate the expression (5.13) with one half the sum of the two possible diagrams. The factor  $\frac{1}{2}$  turns out to be important.

It is obvious that Fig. 5 is not a skeleton diagram and is of just the form that had to be omitted in the construction of reduced graphs of order  $p=2$ . This point suggests that we look for the expected cancellation of (5.13) among the second-order diagrams. Consider, for example, the diagram shown in Fig. 6. The contribution to  $\sigma$  from the intermediate state containing two pairs is, to order  $T^2$ ,

$$\begin{aligned}
 & -\frac{\pi\beta}{3\Omega} \int \int \int \int d\xi_1 d\xi_2 d\xi_3 d\xi \\
 & \quad \times \delta(\xi_1 + \xi_2 - \xi_3 - \xi) f^+(\xi_1) f^+(\xi_2) f^-(\xi_3) f^-(\xi) \\
 & \quad \times \lim_{T \rightarrow 0} \sum_{\text{mom., spins}} \mathbf{\Lambda}^{(1)}(\mathbf{k}, \mu) \cdot \mathbf{\Lambda}^{(1)*}(\mathbf{k}+\mathbf{q}, \mu) \\
 & \quad \times \langle S(\mathbf{k}, \mu) \rangle \langle S^*(\mathbf{k}+\mathbf{q}, \mu) \rangle |\mathbf{T}|^2 \langle \mathcal{G}_{\mathbf{k}}(\mu) \rangle \\
 & \quad \times \langle \mathcal{G}_{\mathbf{k}+\mathbf{q}}(\mu) \rangle \langle \mathcal{G}_{\mathbf{k}'}(\mu) \rangle \langle \mathcal{G}_{\mathbf{k}'-\mathbf{q}}(\mu) \rangle. \quad (5.15)
 \end{aligned}$$

The similarity of (5.15) to (5.13) should be apparent. In evaluating (5.15) to lowest order in  $\Gamma_{\text{imp}}$ , we may make the approximations:

$$\begin{aligned}
 \langle S(\mathbf{k}, \mu) \rangle \langle \mathcal{G}_{\mathbf{k}}(\mu) \rangle &= \frac{\Gamma_{\text{imp}} (\epsilon_{\mathbf{k}} - \mu - \Delta + i\Gamma_{\text{imp}})}{\pi [(\epsilon_{\mathbf{k}} - \mu - \Delta)^2 + \Gamma_{\text{imp}}^2]^2} \\
 &\cong \frac{i}{2\Gamma_{\text{imp}}} \delta[\epsilon_{\mathbf{k}} - \mu - \Delta(\mathbf{k}, \mu)] \quad (5.16)
 \end{aligned}$$

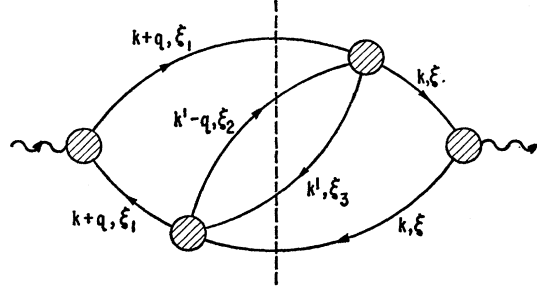


FIG. 6. A special skeleton diagram which yields a second-order reduced graph.

and

$$\begin{aligned}
 & \langle S^*(\mathbf{k}+\mathbf{q}, \mu) \rangle \langle \mathcal{G}_{\mathbf{k}+\mathbf{q}}(\mu) \rangle \\
 & \cong -\frac{i}{2\Gamma_{\text{imp}}} \delta[\epsilon_{\mathbf{k}+\mathbf{q}} - \mu - \Delta(\mathbf{k}+\mathbf{q}, \mu)]. \quad (5.17)
 \end{aligned}$$

Notice that here we have two factors  $\frac{1}{2}$  as opposed to the single factor  $\frac{1}{2}$  which appears on the left-hand side of Eq. (5.12) in connection with the expression (5.13). This extra factor of  $\frac{1}{2}$  which occurs in the evaluation of diagrams of the form of Fig. 6 is exactly right to make up for the  $\frac{1}{2}$  which we attributed to diagram counting at the end of the last paragraph. In other words, the diagrams of Figs. 5 and 6 make  $T^2$  contributions to  $\sigma$  which are directly comparable.

We examine now the sum of all reduced diagrams of order  $p=2$  which may be formed using only the special vertex graphs drawn in Fig. 7. These graphs have the common feature that each may be separated into two parts,  $\mathbf{\Lambda}^{(1)}$  and  $\mathbf{T}$ , by cutting only a single electron line. It follows from the discussion of the last paragraph that we are now allowed to form all combinations of these

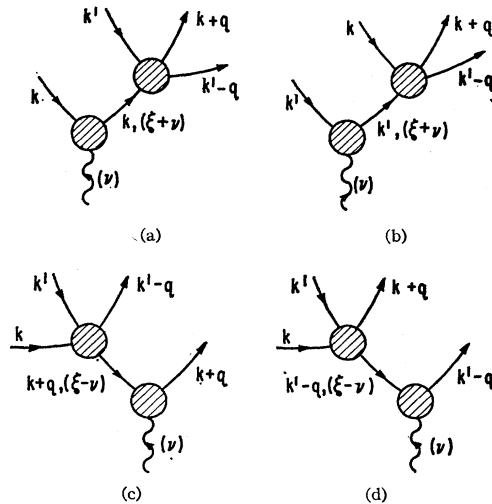


FIG. 7. The special vertex graphs which participate in the cancellation of a spurious  $T^2$  correction to the conductivity.

vertex diagrams without regard to whether the result is skeleton-like or not. For example, Fig. 5 may be constructed by combining Fig. 7(a) with its time-reverse. By combining 7(c) with the time-reverse of 7(a) we form Fig. 6. Each of the graphs in Fig. 7 contributes a factor of the form

$$\pm T \frac{i}{2\Gamma_{\text{imp.}}} \mathbf{\Lambda}^{(1)} = \pm T \frac{i}{2\tilde{\Gamma}_{\text{imp.}}} \mathbf{J}, \quad (5.18)$$

where  $\tilde{\Gamma}_{\text{imp.}} = N\Gamma_{\text{imp.}}$  is the true relaxation rate and  $\mathbf{J} = N\mathbf{\Lambda}^{(1)}$  is the current of a quasi-particle as discussed in II. The sign  $\pm$  must be determined by returning to Eq. (3.52) where we gave  $\nu$  a small imaginary part before letting it vanish. Now the single explicit internal electron lines in Figs. 7(a) and 7(b) may be labeled by an energy variable  $\xi + \nu$ ; whereas the corresponding lines in Figs. 7(c) and 7(d) must carry an energy  $\xi - \nu$ . The sign of the  $\nu$  in the energy variable determines whether the propagator is to be evaluated just above or just below the real axis, and, according to Eq. (5.4), whether  $\Gamma$  appears with a  $+$  or  $-$  sign. It follows that the vertex graphs 7(a) and 7(b) carry a sign opposite to that of 7(c) and 7(d). The sum of all four graphs then contains a factor

$$\mathbf{J}_{\mathbf{k}} + \mathbf{J}_{\mathbf{k}'} - \mathbf{J}_{\mathbf{k}+\mathbf{q}} - \mathbf{J}_{\mathbf{k}'-\mathbf{q}} = 0, \quad (5.19)$$

which vanishes because current must be conserved in the scattering event described by  $T$ . This proves the desired cancellation and eliminates the spurious  $T^2$  correction in  $\bar{\sigma}^{(1)}$ .

The remaining reduced graphs of order  $p=2$  must be constructed with vertex functions  $\mathbf{\Lambda}^{(2)}$  formed by inserting the external interaction line only into internal lines of the scattering amplitude  $T$ . With this restriction it is impossible to construct anything but skeleton diagrams with arbitrary combinations of the vertex graphs. Thus we may sum all diagrams by inserting at each vertex in the reduced graph the sum of all vertex functions. Denote this sum by  $\mathbf{\Lambda}^{(2)'}$ . Furthermore, the singularities associated with the four lines in the reduced graph no longer can reappear in  $\mathbf{\Lambda}^{(2)'}$ . In contrast to Eqs. (5.16) and (5.17), we now may use the approximation

$$\langle \mathcal{O}_{\mathbf{k}}(\mu) \rangle \cong \delta[\epsilon_{\mathbf{k}} - \mu - \Delta(\mathbf{k}, \mu)] \quad (5.20)$$

for each of the lines in the reduced diagram. The net  $T^2$  contribution from reduced graphs of order  $p=2$  is

$$\begin{aligned} \bar{\sigma}^{(2)} = & -\frac{\pi\beta}{6\Omega} \int \int \int d\xi_1 d\xi_2 d\xi_3 d\xi_4 \\ & \times \delta(\xi_1 + \xi_2 - \xi_3 - \xi_4) f^+(\xi_1) f^+(\xi_2) f^-(\xi_3) f^-(\xi_4) \\ & \times \lim_{T \rightarrow 0} \sum_{\text{mom., spins}} |\mathbf{\Lambda}^{(2)'}|^2 \langle \mathcal{O}_{\mathbf{k}}(\mu) \rangle \langle \mathcal{O}_{\mathbf{k}'}(\mu) \rangle \\ & \times \langle \mathcal{O}_{\mathbf{k}+\mathbf{q}}(\mu) \rangle \langle \mathcal{O}_{\mathbf{k}'-\mathbf{q}}(\mu) \rangle. \end{aligned} \quad (5.21)$$

By virtue of (5.20),  $\bar{\sigma}^{(2)}$  is finite in the limit  $\Gamma_{\text{imp.}} \rightarrow 0$ , and need not be included in our final expression for the conductivity.

The fact that the second-order reduced graphs do not contribute to the dc conductivity to lowest order in the impurity concentration suggests the following physical interpretation of these higher-order terms. Apparently Eq. (5.21) describes a contribution to the conductivity associated with a correlated pair of quasi-particles. That is, during the time in which two quasi-particles are in interaction, the pair plays the role of a new kind of current carrier. In a normal Fermi fluid, however, the pair correlation persists only for a finite time; thus the pair current decays spontaneously even in the absence of impurities. As long as the pair correlation time is short compared to  $\tilde{\Gamma}_{\text{imp.}}^{-1}$ , we may expect (5.21) to make a negligible contribution to  $\sigma$ . On the other hand, a resonance in the scattering amplitude  $T$  near the Fermi surface might cause  $\mathbf{\Lambda}^{(2)'}$  to become large; and a bound-state pole might be disastrous. In fact, Thouless has shown that the appearance of a bound-state pole in  $T$  is directly related to the phenomenon of superconductivity.<sup>20</sup>

#### ACKNOWLEDGMENTS

The author wishes to acknowledge a Ford Foundation grant for study and research which he received at Carnegie Institute of Technology, where this work was begun. This paper was completed at the University of California, San Diego, with support from a National Science Foundation Fellowship. Special thanks are due to Professor J. M. Radcliffe for his help and participation in this investigation.

<sup>20</sup> D. J. Thouless, Ann. Phys. (New York) **10**, 553 (1960).